Induction of Alzheimer's disease pathology by early-life stress

Tomoko Tanaka[1], Shinobu Hirai [1], Masato Hosokawa [2], Takashi Saito [3,4], Hiroshi Sakuma [5], Takaomi Saido [3], Masato Hasegawa [2], Haruo Okado [1, *]

[1] Laboratory of Neural Development, Department of Psychiatry & Behavioral Science, Tokyo Metropolitan Institute of Medical Science, Tokyo, Japan.

[2] Dementia Research Project, Department of Brain & Neuroscience, Tokyo Metropolitan Institute of Medical Science, Tokyo, Japan.

[3] Laboratory for Proteolytic Neuroscience, RIKEN Center for Brain Science, Saitama, Japan.

[4] Department of Neurocognitive Science, Institute of Brain Science, Nagoya City University Graduate School of Medical Science, Nagoya, Japan.

[5] Child brain Project, Department of Brain & Neuroscience, Tokyo Metropolitan Institute of Medical Science, Tokyo, Japan.

* Correspondence should be addressed to Haruo Okado, Neural Development Project, Department of Brain Development and Neural Regeneration, Tokyo Metropolitan Institute of Medical Science, Tokyo 156-8506, Japan. E-mail: okado-hr@igakuken.or.jp (H.O.)

Competing interests

The authors declare that the research was conducted in the absence of any commercial or financial relationships that could be construed as a potential conflict of interest.

Abstract

Alzheimer's disease (AD), a progressive neurodegenerative disorder, is a serious social problem. Recently, several early-life factors have been associated with an increased risk of a clinical diagnosis of AD. In the present study, we investigated the involvement of early-life stress in AD pathogenesis using heterozygous APP mutant mice ($App^{NL\text{-}G\text{-}F/wt}$) and wild-type ($App^{wt/wt}$) mice. Maternal separation was used as an animal paradigm for early-life stress. We found that stressed $App^{wt/wt}$ mice showed narrowing of vessels and decreased pericyte coverage of capillaries in prefrontal cortex, while stressed $App^{NL\text{-}G\text{-}F/wt}$ mice showed impairment of place memory, and earlier formation of Aβ plaques and disruption of the blood–brain barrier than non-stressed $App^{NL\text{-}G\text{-}F/wt}$ mice. We detected severe activation of microglia in the stressed $App^{NL\text{-}G\text{-}F/wt}$ mice and stressed $App^{wt/wt}$ mice. In the earlier stage, we detected morphological change and functional change in microglia in the stressed $App^{NL\text{-}G\text{-}F/wt}$ mice and stressed $App^{wt/wt}$ mice, and also detected morphological change in the microglia in the non-stressed $App^{NL\text{-}G\text{-}F/wt}$ mice. Therefore, we hypothesize that activated microglia induced by the combination of maternal separation and APP mutation impairs the vascular system, leading to AD progression. These findings therefore suggest that maternal separation causes early induction of AD pathology.

Introduction

The development of abnormal physiology in association with increased age is observed in the progression of many disorders. Although genetic and environmental factors do influence life-span, daily habits and environmental stresses such as alcohol intake and diet have the major influence on life-span, rather than genetic factors (1). Acceleration of the aging process by such environmental factors is thought to increase both the risk of developing a disease and mortality from a disease. Alzheimer's disease (AD) is one such disease that is thought to be influenced by environmental factors; it is characterized by progressive impairment of cognitive functions such as memory. It is considered that the acquired predisposition to AD increases with age, and that trauma during adulthood increases the likelihood of developing AD. Moreover, recent epidemiological research has suggested that stressful environmental factors during the developmental period, including mistreatment, neglect, and the loss of a parent, can also increase the likelihood of developing AD (2-4). However, as the research behind these findings is generally the result of retrospective cohort studies, it is unclear whether early-life stress affects the onset and progression of AD.

Recently, it was demonstrated that vascular impairment, which can be recognized as a

postmortem pathological finding in the brain, is detected before the onset of AD. Therefore, vascular impairment is noted as an initial symptom of AD (5-8). The neurovascular unit (NVU) is a concept consisting of neurons, endothelial cells, pericytes, microglia, and astrocytes. As the NVU is important for the extrusion of amyloid beta, an impairment in extraction can cause sporadic AD and cerebral amyloid angiopathy (9). In particular, the capillary vessels in the brain play an important role in the extrusion of amyloid beta. Dysfunction of the blood–brain barrier (BBB) and a following decrease in amyloid beta clearance through the cerebral vascular system is recognized in AD. It was demonstrated that degeneration of cells making up the BBB, such as pericytes, cause dysfunction of the BBB (10). However, it remains unclear how early-life stress can result in dysfunction of the vascular system.

In this study, we investigated whether maternal separation, which can be used as an early-life stress in rodents, facilitates the development of AD, with the purpose of understanding the causal association between the development of AD and early-life stress. Having found indications that maternal separation affects the development of AD, we then investigated the potential changes induced by maternal separation, paying particular attention to capillary vessel morphology in heterozygous APP mutant mice ($App^{NL\text{-}G\text{-}F/wt}$) and wild-type ($App^{wt/wt}$) mice. As a

result, we established that maternal separation facilitates the development of AD. Furthermore, we found that impairment of capillaries, probably caused by abnormalities in microglia, leads to dysfunction of the BBB, which facilitates development of clinical AD.

Results

Experimental design

Figure 1A shows the experimental schedule. To investigate whether stress in the early developmental stage is involved in the onset and/or progression of AD, we performed maternal separation for 3 hours daily during the period from postnatal day (P)2 to P15 in *App*$^{wt/wt}$ and *App*$^{NL\text{-}G\text{-}F/wt}$ mice, which show an AD-like phenotype in the late-aged stage. We then performed behavioral tests and tissue sampling around P45 and P120.

Maternal separation induced impairment of object location memory and fear contextual memory in App$^{NL\text{-}G\text{-}F/wt}$ *mice*

Figure 1B illustrates the effect of maternal separation on object location memory. Object location memory in the adult *App*$^{wt/wt}$ mice was not altered by postnatal maternal separation, as indicated by the fact that the discrimination index was not changed by maternal separation. By contrast, object location memory in the adult *App*$^{NL\text{-}G\text{-}F/wt}$ mice was impaired by postnatal maternal separation, as indicated by a discrimination index close to zero. The discrimination index for the non-stressed *App*$^{NL\text{-}G\text{-}F/wt}$ mice showed intact object location memory. The result of

two-way ANOVA indicates that genotype and maternal separation interact on object location memory. Figure 1C indicates the effect of maternal separation on contextual and cued fear memory. Contextual fear memory in the adult $App^{wt/wt}$ mice was not altered by maternal separation, while that in the adult $App^{NL\text{-}G\text{-}F/wt}$ mice was impaired by maternal separation, as indicated by the lower freezing time in the stressed $App^{NL\text{-}G\text{-}F/wt}$ mice in comparison with the non-stressed $App^{NL\text{-}G\text{-}F/wt}$ mice and non-stressed $App^{wt/wt}$ mice. By contrast, tone-cued fear memory was not impaired in any of the four groups, indicating that contextual memory, which is related to prefrontal cortex–hippocampus signaling and is known to be necessary for the encoding of spatial cues, was impaired.

Maternal separation facilitates the formation of amyloid beta plaque in heterozygous APP mutant mice

Figure 2A indicates the effect of postnatal maternal separation on the formation of amyloid beta plaque. The formation of amyloid beta plaque in the $App^{NL\text{-}G\text{-}F/wt}$ mice was higher in those mice that underwent postnatal separation than in those that did not. Figure 2B illustrates the relationship between the sizes of the amyloid beta plaques and the distances from the amyloid

beta plaques to vessels in the stressed and non-stressed *App*$^{NL\text{-}G\text{-}F/wt}$ mice who had mild amyloid beta plaque symptoms. The correlations between the sizes of amyloid beta plaques and the distances from the amyloid beta plaques to vessels were significant, which suggests the possibility that amyloid beta plaque was generated from the vessels.

Post-natal maternal separation induces vascular system impairment in adult mice

Figure 3 illustrates the effect of maternal separation on the vascular system. The stressed *App*$^{wt/wt}$ and stressed *App*$^{NL\text{-}G\text{-}F/wt}$ mice showed lower pericytes coverage of capillaries in the prefrontal cortex (PFC) than the unstressed controls (Figure 3A). The lower pericyte coverage of capillaries is involved in BBB leakage and observed in AD pathology (11). Furthermore, post-natal maternal separation induced a narrowing of capillary diameter in both the *App*$^{wt/wt}$ mice and *App*$^{NL\text{-}G\text{-}F/wt}$ mice. However, extra-vascular accumulation of fibrinogen deposits in the PFC was detected in only the stressed *App*$^{NL\text{-}G\text{-}F/wt}$ mice (Figure 3D). We speculate that this accumulation was caused by leakage of fibrinogen due to impairment of the vascular system in only the stressed *App*$^{NL\text{-}G\text{-}F/wt}$ mice. Phenotypes showing decreased pericyte coverage, a narrowing of capillary diameter, and impairment of the BBB are frequently observed in AD

patients (11).

Either post-natal maternal separation or APP mutation caused activation of and morphological change in microglia in adult mice

As the vascular system is affected by microglia, we examined the activity and morphology of the microglia. Figure 4 indicates the effects of postnatal maternal separation on microglia. The maternal separation caused activation of the microglia in the PFC of both $App^{wt/wt}$ mice and $App^{NL\text{-}G\text{-}F/wt}$ mice (Figure 4A). Although the numbers of microglia were not significantly different between each group, except for the microglia on the amyloid beta plaque, the proportions of soma and dendrites, which are stained by Iba1, were lower in both the phenotype groups that were subjected to maternal separation (Figure 4A) in comparison with the corresponding controls. The result of two-way ANOVA indicated that there may be morphological change in both genotypes by maternal separation. More detailed analysis of morphological change revealed differences between each group. Lower numbers of dendrite terminals and a shortening of the total branch length were detected in the stressed $App^{NL\text{-}G\text{-}F/wt}$ mice in comparison with the non-stressed controls. In the $App^{wt/wt}$ mice, the mice subjected to

maternal separation also showed lower numbers of dendrite terminals and shortening of the total branch length in comparison with non-stressed controls. On the other hand, the number of dendrite terminals was lower in the non-stressed *App*$^{NL\text{-}G\text{-}F/wt}$ mice than in the non-stressed *App*$^{wt/wt}$ mice, although the difference was not significant (Figure 4B). The non-stressed *App*$^{NL\text{-}G\text{-}F/wt}$ mice may show mild microglial symptoms compared with the stressed animals. Furthermore, higher quantities of vessel-associated microglia, which play an important role in the vascular system, were detected in the stressed *App*$^{NL\text{-}G\text{-}F/wt}$ mice in all groups. In the *App*$^{wt/wt}$ mice, vessel associated microglia tended to be higher in the mice subjected to maternal separation than in the non-stressed controls. Furthermore, in the non-stressed *App*$^{NL\text{-}G\text{-}F/wt}$ mice, the level of vessel associated microglia tended to be higher than in non-stressed *App*$^{wt/wt}$ mice (Figure 4C), suggesting strengthening of the interaction between microglia and vessels.

The stressed App$^{wt/wt}$ *and App*$^{NL\text{-}G\text{-}F/wt}$ *mice showed intact object location memory, absence of amyloid beta plaque, and normal vascular morphology and pericyte in adolescence*

To detect initial changes in the stressed and/or mutated mice, we examined the phenotypes at an earlier stage (P90), that is, in adolescence. Figure 5A illustrates the effect of postnatal

maternal separation on object location memory in adolescence. In all groups, the discrimination index for object location memory indicated object location memory to be intact. Figure 5B indicates the absence of amyloid beta plaque in all groups. Figure 5C shows that there was no impairment of vascular morphology and pericytes in any of the groups.

Postnatal maternal separation and APP mutation cause functional and morphological change to microglia in adolescence

Figure 5 indicates the effect of postnatal maternal separation on microglia in adolescence. The numbers of activated microglia were not significantly different between each group (Figure 6A); however, the proportions of soma and dendrites, which are stained by Iba1, were lower in the maternally separated groups in both genotypes (Figure 6A). There may be morphological change in both phenotypes by maternal separation. A more detailed analysis of morphological differences revealed lower numbers of dendrite terminals in the stressed $App^{NL\text{-}G\text{-}F/wt}$ mice than in the non-stressed $App^{wt/wt}$ mice. In the $App^{wt/wt}$ mice, the maternally separated mice also showed lower numbers of dendrite terminals. Furthermore, lower numbers of dendrite terminals were detected in the non-stressed $App^{NL\text{-}G\text{-}F/wt}$ mice than in the non-stressed $App^{wt/wt}$ mice (Figure

6B). On the other hand, the numbers of vessel-associated microglia did not differ between the groups (Figure 6C). To evaluate microglial function, we measured the level of TNF-R1 protein in the PFC. Stressed $App^{wt/wt}$ and $App^{NL\text{-}G\text{-}F/wt}$ mice showed higher levels of TNF-R1 protein than the unstressed mice (Figure 6D). We could detect initial changes associated with both maternal separation and heterozygotic mutation in adolescence, indicating the possibility that a change in microglia caused by both maternal separation and APP mutation induces an AD-like phenotype. To assess the effect on the hypothalamus-pituitary-adrenal axis, we measured serum corticosterone levels in unstressed and stressed mice. Stressed $App^{NL\text{-}G\text{-}F/wt}$ mice showed more corticosterone release than unstressed mice (Figure 6E).

Discussion

In this study, we investigated whether postnatal maternal separation facilitates the development of AD, with the aim of understanding the causal association between early-life stress and the development and progression of AD. We also investigated for changes induced by maternal separation, particularly in capillary vessels. We established that postnatal maternal separation facilitates the impairment of spatial cognitive function and the formation of amyloid beta plaque in *App*$^{NL\text{-}G\text{-}F/wt}$ mice, with disruption of micro-capillaries, and we verified that early-life stress constitutes a risk factor for AD. Furthermore, we found that morphological and functional changes to microglia are early symptoms in our experimental model, and suggest the possibility that impairment of the cerebral vascular system caused by interactions between microglia and vasculature induces dysfunction in the BBB, thereby facilitating the clinical condition of AD.

Research using the Childhood Trauma Questionnaire to assess childhood stress has suggested that early-life stress may be associated with increased risk of AD and dementia (3). However, because most previous reports, including the above research, were based on retrospective cohort studies, it remains unclear whether early-life stress affects the onset and progression of AD.

Although it has been reported that maternal separation facilitates the formation of amyloid beta plaque using an AD mouse model different from the one we used (12), the pathway by which maternal separation induces increased amyloid beta plaque remains unclear. We found that maternal separation facilitates the impairment of spatial cognitive function and the formation of amyloid beta plaque through impairment of the cerebral vascular system in *App*$^{NL\text{-}G\text{-}F/wt}$ mice. We propose that these maternally separated *App*$^{NL\text{-}G\text{-}F/wt}$ mice can be used as a stress-induced AD mouse model. As it is known that progression of AD in humans is exacerbated by stress, such as a change in abode and hospital admission in old age, our AD mouse model may contribute to understanding the mechanism of stress-induced AD and how it can be prevented.

We found that both maternal separation and genetic factors induced impairment of the cerebral capillary vascular system to a mild degree. However, dysfunction of the BBB, which is a more serious symptom, was detected in the stressed *App*$^{NL\text{-}G\text{-}F/wt}$ mice and was related to both early-life stress and genetic factors. Furthermore, from our results showing that primary amyloid beta plaque assembles around vessels, we speculate that impairment of the cerebral capillary vascular system plays a role in AD pathology. Our results support the hypothesis linking cerebral vascular disease to AD.

We report that postnatal maternal separation induces impairments to the cerebral vascular system, with impairments to pericytes and the narrowing of vessels in adulthood. Both of these phenotypes are detected in the postmortem brains of human patients with AD (11). Therefore, these findings indicate the relationship between early-life stress and AD pathology. It has been demonstrated that both antenatal and postnatal stress delay the development of the BBB, while the BBB matures at the time of weaning (13). We also detected no impairment in vascular morphology or in pericytes in adolescence. Our findings that early-life stress induces impairments in adult mice is in accord with the Development Origins of Health and Disease (DOHaD) hypothesis, which purports that exposure to certain environmental conditions during critical periods of development and growth may have significant adverse effects on short- and long-term health. However, we found that fibrinogen accumulated on vascular walls in the non-stressed App$^{NL\text{-}G\text{-}F/wt}$ mice, indicating impairment of the cerebral vascular system. As the ultrastructural breakdown of capillaries and a decrease in blood flow are detected in AD patients and AD mouse models (14), it is likely that impairment of the cerebral vascular system develops before the onset of AD pathogeny in non-stressed *App*$^{NL\text{-}G\text{-}F/wt}$ mice.

We detected morphological changes in microglia and changes in their pro-inflammatory

properties (which are mediated by the activation of TNF-R1) at an early stage, when we did not detect amyloid plaque formation, changes to the vascular system, or changes in behavior. It is reported that microglia show morphological changes in response to the clinical condition of AD (15). Although it has been demonstrated that maternal separation induces the activation of microglia, it is often the case that such research focuses on the alteration of microglia immediately after stress (16). However, it has also been demonstrated that maternal separation induces an increase in the phagocytic capacity of microglia in adolescence. An increase in corticosterone in response to stress has been reported to be related to a change in the microglia (17). Our stress-induced AD mouse model also showed the enhancement of corticosterone release in response to isolation stress. In fact, the production of corticosterone in response to stress facilitates the release of monocytes into the circulation from bone marrow, which in turn facilitates monocyte adherence to vessels (18). It has been demonstrated that these released monocytes upregulate IL-1β and stimulate endothelial cells (19). Haruwaka et al. hypothesized that endothelial cells may respond to systemic inflammation and release molecules to trigger microglia migration and phenotype changes, and they indicated that chemokine (C-C motif) ligand 5 (CCL5), which is secreted by endothelial cells, induces the attraction of microglia to

vessels (20). Recently, it was demonstrated that plasma from aged mice affected the activity of microglia, referred to as neuroinflammation, and for endothelial cell, which is the major cell type of BBB, in young mice (21). The authors suggested that circulating cytokines and chemokines with detrimental effects on the brain give rise to the above phenomenon. Considering that increased age is crucial for the development of AD, these inflammatory signals in the plasma may induce AD. There is the possibility that early-life stress such as maternal separation affects the immune system and enhances the generation of these inflammatory signals in the plasma in early adulthood. On the other hand, activation of the NOD-like receptor (NLR) pyrin domain-containing 3 (NLRP3) inflammasome is induced by soluble amyloid beta oligomer, and results in the activation of caspase-1 and the release of pro-inflammatory cytokines (22). The activation of NLRP3 in microglia results in amyloid beta plaque accumulation and cognitive dysfunction (23). The APP mutation, which increases amyloid beta production, affects the immune system, as revealed by the activation and morphological alteration of microglia through different pathways during early-life stress.

Post-natal maternal separation can induce an increase in the motility of microglia in the sensory motor cortex in adult mice (24), although the physiological mechanism responsible for

the increased motility remains to be identified. Microglia with increased mobility may be able to detect impairment of the vascular system. In the present study, maternal separation or genetic factors resulted in the microglia being attracted to vessels. Furthermore, the combination of maternal separation and genetic factors led to further attraction of microglia to vessels. As the non-stressed *App*$^{NL\text{-}G\text{-}F/wt}$ mice also showed morphological change in adolescence, our data support the hypothesis that impairment of the vascular system by amyloid beta oligomer induces activation of microglia (25). As microglia and the vascular system are deeply linked, the possibility that an undetectable alteration of the vascular system led to a change in the microglia, which then led to the development of AD via an interaction between microglia and the vascular system, cannot be ruled out. In the future, we deem it desirable to investigate the presence or absence of impairments to the vascular system using simultaneous in vivo imaging of microglia and vessels. As the activation of microglia by maternal separation may differ in character from that caused by genetic factors, further investigation is needed.

There are several limitations to the present study. The first is that maternal separation induces both physical and psychological stress. We cannot say for sure which of these stresses results in the development of AD after adulthood. Furthermore, we cannot be certain that maternal

separation reflects early-life stress. However, it is clear that environmental factors during early life can lead to a potential change, and that the effect becomes noticeable after reaching adulthood. Second, it is uncertain how closely our AD mouse model reflects human patients with AD, which is a common issue with animal models. Our stress-induced AD mouse model shows symptoms including the impairment of hippocampus-dependent cognitive function, accumulation of amyloid beta plaque, and impairment of the vascular system. We believe that it will be important to make efficient use of these mice in the further study of AD.

In the present study, we established that maternal separation facilitates the development of AD. Furthermore, we identified changes in microglia induced by maternal separation and/or genetic factors as an early phenotype, which probably preceded the impairment of the vascular system in the stress-induced AD mouse model. These results indicate that microglia could have potential use as biomarkers and as targets for new therapies against AD.

1 Materials and methods

2 All experimental procedures were approved by the Animal Experimentation Ethics

3 Committee of the Tokyo Metropolitan Institute of Medical Science (49040).

4

5 *Animals*

6 The original lines of App mutant mice ($App^{NL\text{-}G\text{-}F/NL\text{-}G\text{-}F}$) were established as a C57BL/6J

7 congenic line (a genetic background strain) by repeated back-crosses, as described previously,

8 and were obtained from RIKEN Center for Brain Science (Wako, Japan) (26). All experiments

9 were performed with heterozygous APP mutant mice ($App^{NL\text{-}G\text{-}F/wt}$) and wild-type mice ($App^{wt/wt}$).

10 All mice were maintained under a 12:12 h light/dark cycle (lights on at 8:00 AM). All efforts

11 were made to minimize the number of animals used and their suffering. All experiments, except

12 for maternal separation, were performed in adolescence (P 45) or adulthood (P90–P120).

13

14 *Maternal separation*

15 Maternal separation is usually used as a form of early-life stress in mice. Pups were separated

16 from their mother for 3 hours daily from P2 to P15. The separated pups were taken to a different

room and placed on a heat pat to maintain their body temperature. The control mice had no experience of maternal separation. The body weights were not significantly different between the control and stressed mice at several stages of development.

Behavioral assessment

Mice were allowed to habituate in the behavioral room for at least 1 hour before commencement of the behavioral test.

The object location test consisted of three phases. All phases were performed under a light intensity of 10 lux. On day 1, the animals were placed in an empty square box for 10 minutes. On day 2, the animals were placed in the same box for 10 minutes with two identical unfamiliar objects. On day 3, the animals were placed in the same box, with one of the two items being displaced to a novel location in the area. The discrimination index was calculated as the ratio of the time spent exploring the novel place to that spent exploring the familiar place: discrimination index = (novel place exploration time – familiar place exploration time)/(novel place exploration time + familiar place exploration time). On each day, the exploration time in

each place was calculated automatically using a DVTrack video tracking system (CompACT VAS/DV; Muromachi, Tokyo, Japan).

The fear conditioning test consisted of three phases. On day 1, the animals were placed in a triangular box for 5 minutes under a light intensity of 30 lux. On day 2, the animals were placed into a conditioning box and were exposed to a 30 second tone and 0.75 mA electric shock three times under a light intensity of 100 lux. On day 3, the animals were placed into the conditioning box for 5 minutes under a light intensity of 100 lux. On day 4, the animals were placed in the same triangular box as used on day 1 for 10 minutes and were exposed to a 30 second tone six times under a light intensity of 100 lux. In each test, the percentage of freezing time and distance travelled (cm) were calculated automatically using ImageFZ software (O'Hara & Co., Tokyo, Japan). Freezing was taken to indicate that the mice remembered the box in which they were exposed to electrical shock.

Immunohistochemistry

At P45 or P120, the mice were anaesthetized with isoflurane and then sequentially perfused through the heart with PBS followed by 4% paraformaldehyde (PFA) in PBS. Their brains were

1 post-fixed, cryoprotected in 20% sucrose at 4℃, and embedded in OCT compound and frozen.
2 Coronal sections of mouse brain were then cut using a cryostat (20 μm). Free-floating sections
3 containing PFC were incubated with mouse anti-human amyloidβ (N) (82E1) Biotin (IBL.,
4 Gunma, Japan), FITC-conjugated tomato-lectin (VECTOR., California, United State), goat anti-
5 aminopeptidase N/CD13 (R&D Systems., Minnesota, United State), rabbit anti-fibrinogen
6 (Agilent., California, United State), rabbit anti-Iba1 (FUJIFILM., Tokyo, Japan), and mouse
7 anti-CD68 (Abcam., Cambridge, United Kingdom), followed by incubation with PBS
8 containing Triton X-100. All primary antibodies were diluted to 1:500 in PBS containing Triton
9 X-100. The sections were then incubated with secondary antibody (Jackson., Maine, United
10 State) (diluted to 1:500 in PBS containing Triton X-100) for 2 hours at room temperature. All
11 sections types were incubated with DAPI (Nacalai Tesque., Kyoto, Japan) for nuclear staining.
12 Fluorescence micrographs of the sections subjected to immunostaining procedures were
13 captured and digitized with a FluoView® FV3000 confocal laser scanning microscope
14 (Olympus., Tokyo, Japan).
15
16 Luminex analysis assay

Following sacrifice, mouse PFC fractions were dissociated with a tissue homogenizer in 100 μl of 0.5 × cell lysis buffer 2 diluted in PBS (R&D Systems). Tissues were lysed at room temperature for 30 minutes, and debris was then removed by centrifugation. Magnetic luminex assays were performed using a Mouse Premixed Multi-Analysis Kit (R&D Systems). Assay procedures were carried out following manufacturer's instructions. Microplates were run on a Bio-Plex 200 system (Bio-Rad., California, United State).

Corticosterone assay

Mice were subjected to isolation stress for 30 mins. Blood samples were taken before stress and immediately after stress and centrifuged at 3,300 rpm to separate serum. Cortisone concentrations were measured using an enzyme-linked immunosorbent assay (ELISA) (AssayPro., Missouri, United State).

Statistical data analysis

Group data are presented as the mean ± SEM. The statistical significance of between-group differences was assessed by Tukey–Kramer test, Dunnett test or two-way ANOVA followed by a

post-hoc Tukey–Kramer test, performed using JMP software (SUS Institute., North Carolina, United State). The interaction between area and distance was assessed by polynomial regression model. The statistical significance of differences between groups and over time was assessed by two-way repeated ANOVA followed by a *post-hoc* Holms test, performed using R software.

Author contributions

T.T. and H.O. designed the research. T.T. performed and analyzed all experiments. T.S. and T.S. generated and provided App mutant mice (*App*$^{NL\text{-}G\text{-}F/NL\text{-}G\text{-}F}$). S.H., M.H., H.S., and M.H. helped with this study and made important suggestions. T.T. generated all the figures and tables and wrote the manuscript. H.O. edited the manuscript and supervised this study.

Acknowledgments

The authors thank Dr. Makoto Hashimoto for advice. We would like to thank bioedit (https://www.bioedit.com/login) for English language editing. This work was partially supported by JSPS KAKENHI Grant Number 18H02537 for Haruo Okado and by JSPS KAKENHI Grant Number 17K16408 for Tomoko Tanaka.

Data availability statement

The datasets analyzed in the present study are available from the corresponding author upon reasonable request.

Requests for materials

Requests for materials should be addressed to Haruo Okado (email: okado-hr@igakuken.or.jp).

References

1. Christensen K, Johnson TE, and Vaupel JW. The quest for genetic determinants of human longevity: challenges and insights. *Nature reviews Genetics.* 2006;7(6):436-48.
2. Seifan A, Schelke M, Obeng-Aduasare Y, and Isaacson R. Early Life Epidemiology of Alzheimer's Disease - A Critical Review. *Neuroepidemiology.* 2015;45(4):237-54.
3. Radford K, Delbaere K, Draper B, Mack HA, Daylight G, Cumming R, et al. Childhood Stress and Adversity is Associated with Late-Life Dementia in Aboriginal Australians. *The American journal of geriatric psychiatry : official journal of the American Association for Geriatric Psychiatry.* 2017;25(10):1097-106.
4. Norton MC, Smith KR, Ostbye T, Tschanz JT, Schwartz S, Corcoran C, et al. Early parental death and remarriage of widowed parents as risk factors for Alzheimer disease: the Cache County study. *The American journal of geriatric psychiatry : official journal of the American Association for Geriatric Psychiatry.* 2011;19(9):814-24.
5. Montagne A, Barnes SR, Sweeney MD, Halliday MR, Sagare AP, Zhao Z, et al. Blood-brain barrier breakdown in the aging human hippocampus. *Neuron.* 2015;85(2):296-302.
6. Montagne A, Nation DA, Pa J, Sweeney MD, Toga AW, and Zlokovic BV. Brain imaging of neurovascular dysfunction in Alzheimer's disease. *Acta Neuropathol.* 2016;131(5):687-707.
7. Iadecola C. The Neurovascular Unit Coming of Age: A Journey through Neurovascular Coupling in Health and Disease. *Neuron.* 2017;96(1):17-42.
8. Wen Y, Yang S, Liu R, and Simpkins JW. Transient cerebral ischemia induces site-specific hyperphosphorylation of tau protein. *Brain research.* 2004;1022(1-2):30-8.
9. Mawuenyega KG, Sigurdson W, Ovod V, Munsell L, Kasten T, Morris JC, et al. Decreased clearance of CNS beta-amyloid in Alzheimer's disease. *Science.* 2010;330(6012):1774.
10. Sweeney MD, Ayyadurai S, and Zlokovic BV. Pericytes of the neurovascular

unit: key functions and signaling pathways. *Nat Neurosci.* 2016;19(6):771-83.

11. Halliday MR, Rege SV, Ma Q, Zhao Z, Miller CA, Winkler EA, et al. Accelerated pericyte degeneration and blood-brain barrier breakdown in apolipoprotein E4 carriers with Alzheimer's disease. *Journal of cerebral blood flow and metabolism : official journal of the International Society of Cerebral Blood Flow and Metabolism.* 2016;36(1):216-27.
12. Hui J, Feng G, Zheng C, Jin H, and Jia N. Maternal separation exacerbates Alzheimer's disease-like behavioral and pathological changes in adult APPswe/PS1dE9 mice. *Behav Brain Res.* 2017;318:18-23.
13. Gomez-Gonzalez B, and Escobar A. Altered functional development of the blood-brain barrier after early life stress in the rat. *Brain Res Bull.* 2009;79(6):376-87.
14. de la Torre JC. Is Alzheimer's disease a neurodegenerative or a vascular disorder? Data, dogma, and dialectics. *The Lancet Neurology.* 2004;3(3):184-90.
15. Yamada J, and Jinno S. Novel objective classification of reactive microglia following hypoglossal axotomy using hierarchical cluster analysis. *J Comp Neurol.* 2013;521(5):1184-201.
16. Roque A, Ochoa-Zarzosa A, and Torner L. Maternal separation activates microglial cells and induces an inflammatory response in the hippocampus of male rat pups, independently of hypothalamic and peripheral cytokine levels. *Brain, behavior, and immunity.* 2016;55:39-48.
17. Rincon-Cortes M, and Sullivan RM. Early life trauma and attachment: immediate and enduring effects on neurobehavioral and stress axis development. *Front Endocrinol (Lausanne).* 2014;5:33.
18. Niraula A, Wang Y, Godbout JP, and Sheridan JF. Corticosterone Production during Repeated Social Defeat Causes Monocyte Mobilization from the Bone Marrow, Glucocorticoid Resistance, and Neurovascular Adhesion Molecule Expression. *The Journal of neuroscience : the official journal of the Society for Neuroscience.* 2018;38(9):2328-40.
19. McKim DB, Weber MD, Niraula A, Sawicki CM, Liu X, Jarrett BL, et al. Microglial recruitment of IL-1beta-producing monocytes to brain

endothelium causes stress-induced anxiety. *Mol Psychiatry.* 2018;23(6):1421-31.

20. Haruwaka K, Ikegami A, Tachibana Y, Ohno N, Konishi H, Hashimoto A, et al. Dual microglia effects on blood brain barrier permeability induced by systemic inflammation. *Nature communications.* 2019;10(1):5816.

21. Yousef H, Czupalla CJ, Lee D, Chen MB, Burke AN, Zera KA, et al. Aged blood impairs hippocampal neural precursor activity and activates microglia via brain endothelial cell VCAM1. *Nat Med.* 2019;25(6):988-1000.

22. Luciunaite A, McManus RM, Jankunec M, Racz I, Dansokho C, Dalgediene I, et al. Soluble Abeta oligomers and protofibrils induce NLRP3 inflammasome activation in microglia. *J Neurochem.* 2019:e14945.

23. Heneka MT, Kummer MP, Stutz A, Delekate A, Schwartz S, Vieira-Saecker A, et al. NLRP3 is activated in Alzheimer's disease and contributes to pathology in APP/PS1 mice. *Nature.* 2013;493(7434):674-8.

24. Takatsuru Y, Nabekura J, Ishikawa T, Kohsaka S, and Koibuchi N. Early-life stress increases the motility of microglia in adulthood. *J Physiol Sci.* 2015;65(2):187-94.

25. Nortley R, Korte N, Izquierdo P, Hirunpattarasilp C, Mishra A, Jaunmuktane Z, et al. Amyloid beta oligomers constrict human capillaries in Alzheimer's disease via signaling to pericytes. *Science.* 2019;365(6450).

26. Saito T, Matsuba Y, Mihira N, Takano J, Nilsson P, Itohara S, et al. Single App knock-in mouse models of Alzheimer's disease. *Nat Neurosci.* 2014;17(5):661-3.

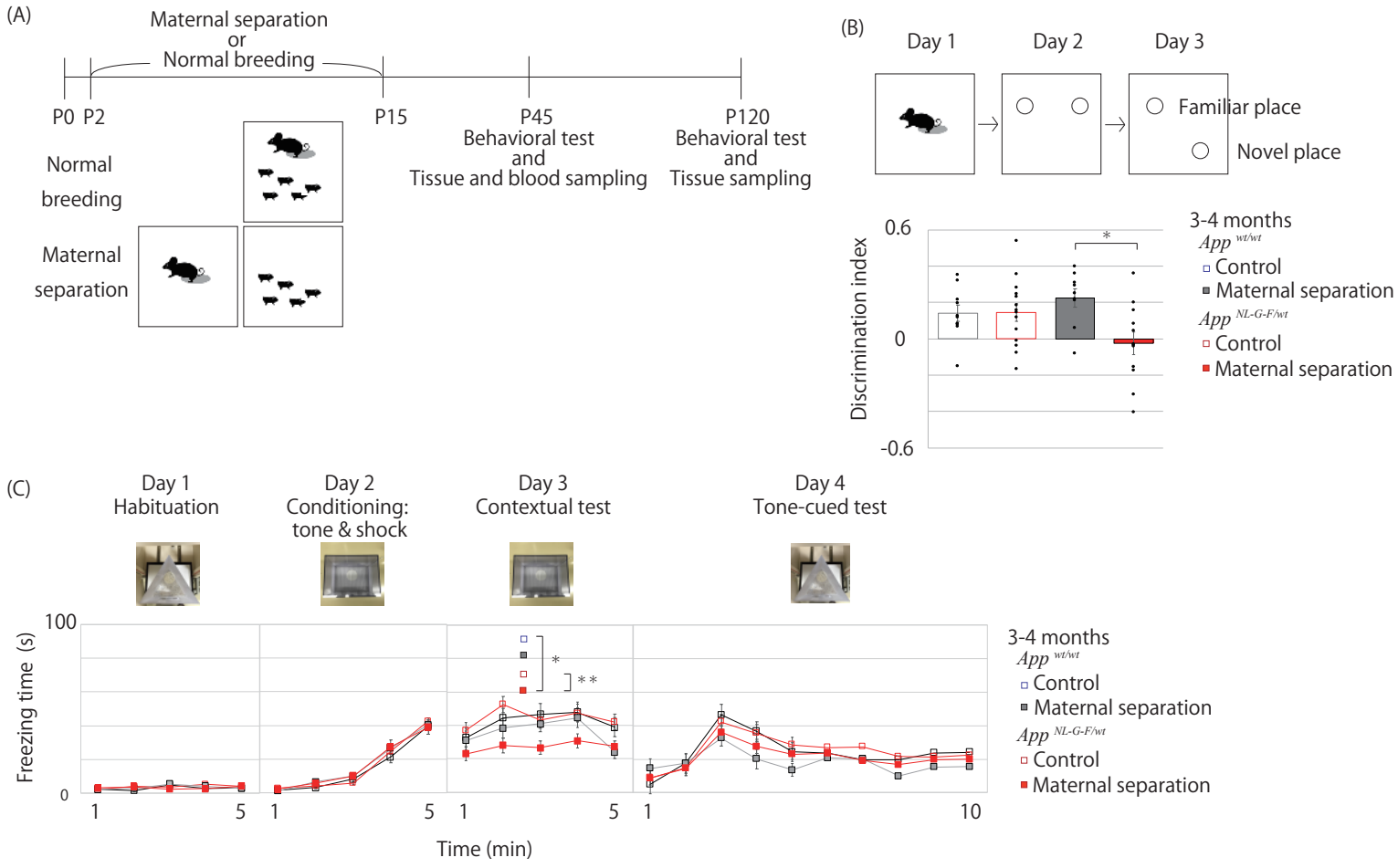

Figure. 1 Maternal separation induces an Alzheimer's disease like behavior.

(A) Time schedule for maternal separation and other investigations. (B) Spatial memory was measured using an object location test. Behavioral layout of the object recognition test for the four experimental groups. Stressed *App*$^{NL\text{-}G\text{-}F/wt}$ mice showed impairment of spatial memory. Main effect of genotype, $F_{(1,41)} = 5.3234$, $p = 0.0262$; main effect of stress, $F_{(1,41)} = 0.6684$, $p = 0.4183$; interaction of genotype × stress, $F_{(1,41)} = 5.8148$, $p = 0.0205$; *$p < 0.05$ stressed *App*$^{NL\text{-}G\text{-}F/wt}$ mice vs stressed *App*$^{wt/wt}$ mice; n = 10/ Non-stressed *App*$^{wt/wt}$ mice , n = 14/ Non-stressed *App*$^{NL\text{-}G\text{-}F/wt}$ mice , n = 9/ Stressed *App*$^{wt/wt}$ mice , n = 12/ Stressed *App*$^{NL\text{-}G\text{-}F/wt}$ mice (two-way ANOVA followed by post-hoc Tukey-Kramer test). (C) Contextual memory and cued memory were measured using a fear-conditioning test. Behavioral layout of the fear conditioning test for the four experimental groups. Stressed *App*$^{NL\text{-}G\text{-}F/wt}$ mice showed impairment of contextual memory. Main effect of group, $F_{(3,73)} = 4.9416$, $p = 0.0035$; main effect of time, $F_{(4,292)} = 5.6188$, $p = 0.0002$; interaction of group × time, $F_{(12,292)} = 0.9194$, $p = 0.5278$; *$p < 0.05$ stressed *App*$^{NL\text{-}G\text{-}F/wt}$ mice vs non-stressed *App*$^{wt/wt}$ mice, **$p < 0.01$ stressed *App*$^{NL\text{-}G\text{-}F/wt}$ mice vs non-stressed *App*$^{NL\text{-}G\text{-}F/wt}$ mice; n = 9/ Non-stressed *App*$^{wt/wt}$ mice , n = 25/ Non-stressed *App*$^{NL\text{-}G\text{-}F/wt}$ mice , n = 9/ Stressed *App*$^{wt/wt}$ mice , n = 25/ Stressed *App*$^{NL\text{-}G\text{-}F/wt}$ mice (two-way repeated ANOVA followed by Holm's test).

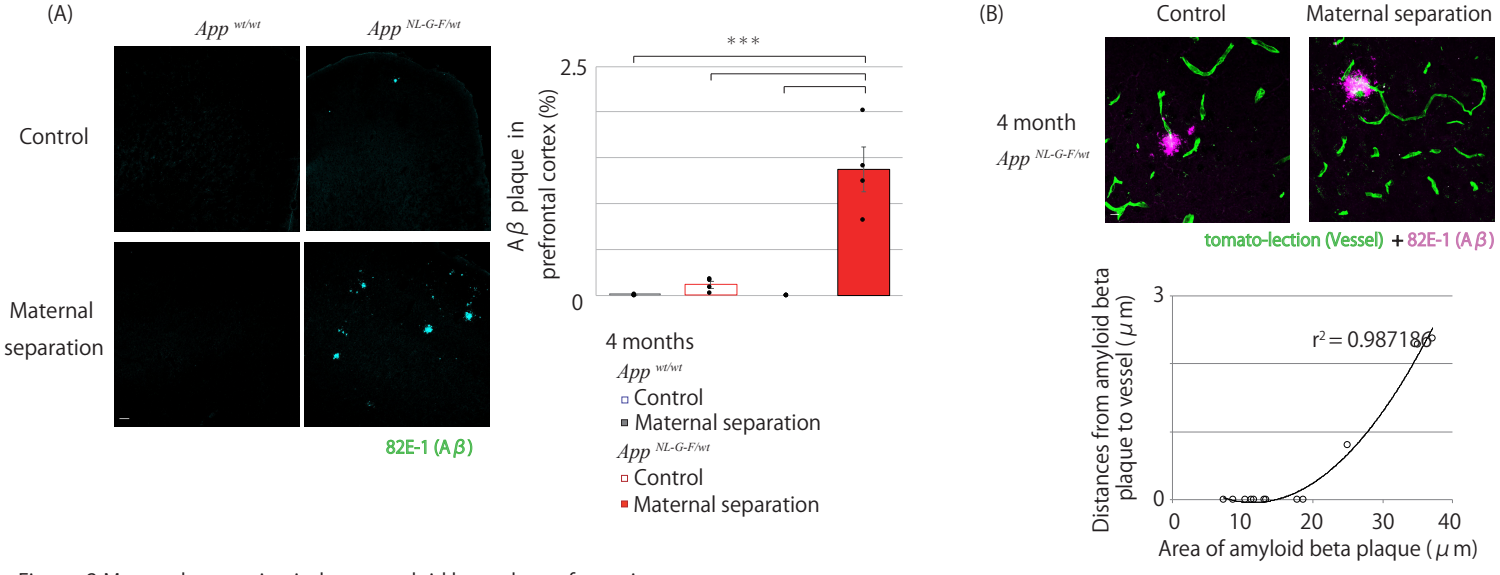

Figure. 2 Maternal separation induces amyloid beta plaque formation.

(A) The formation of amyloid beta plaque detected by 82E1-biotin (cyan). The formation of amyloid beta plaque was facilitated by maternal separation in stressed *App*$^{NL\text{-}G\text{-}F/wt}$ mice. ***$p < 0.001$ stressed *App*$^{NL\text{-}G\text{-}F/wt}$ mice vs other groups n = 4/each group (Tukey-Kramer test). Scale bar = 10 μm.

(B) The distance from the amyloid beta plaques to vessels and the area of amyloid beta plaque was detected by 82E1-biotin (magenta) and tomato-lectin (green). The area of amyloid beta plaque showed a significant association with the distance from the amyloid beta plaque to vessels in non-stressed and stressed *App*$^{NL\text{-}G\text{-}F/wt}$ mice. $r^2 = 0.987186$ $p < 0.001$; n = 12 (polynomial regression). Scale bar = 20 μm.

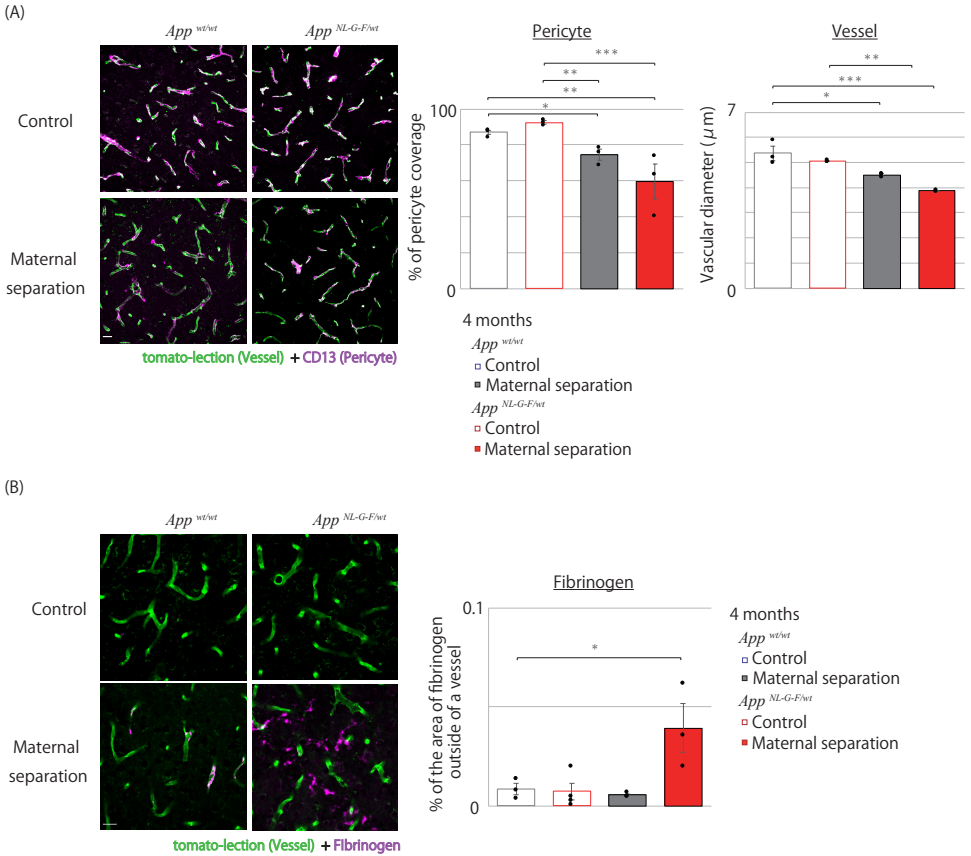

Figure. 3 Maternal separation induced impairment to the vascular system. (A) The health of the vascular system was evaluated by tomato-lectin labelling of endothelial cells (green) and CD13 (magenta) labelling of pericytes. Maternal separation induced lower pericyte coverage in $App^{wt/wt}$ mice and $App^{NL-G-F/wt}$ mice. * $p < 0.05$, stressed $App^{wt/wt}$ mice vs non-stressed $App^{wt/wt}$ mice, ** $p < 0.01$ stressed $App^{NL-G-F/wt}$ mice vs non-stressed $App^{wt/wt}$ mice, ** $p < 0.01$, stressed $App^{wt/wt}$ mice vs non-stressed $App^{NL-G-F/wt}$ mice, *** $p < 0.001$ stressed $App^{NL-G-F/wt}$ mice vs non-stressed $App^{NL-G-F/wt}$ mice. Furthermore, maternal separation also induced a narrowing of vascular diameter in both phenotypes. * $p < 0.05$ stressed $App^{wt/wt}$ mice vs non-stressed $App^{wt/wt}$ mice, *** $p < 0.001$ stressed $App^{NL-G-F/wt}$ mice vs non-stressed $App^{wt/wt}$ mice, ** $p < 0.01$ stressed $App^{NL-G-F/wt}$ mice vs non-stressed $App^{NL-G-F/wt}$ mice; n = 3/each group (Tukey-Kramer test). Scale bar = 20 μm. (B) The integrity of the BBB was evaluated by tomato-lectin labelling of endothelial cells (green) and fibrinogen (magenta). Maternal separation induced an accumulation of fibrinogen outside of vessels in stressed $App^{NL-G-F/wt}$ mice. * $p < 0.05$ stressed $App^{NL-G-F/wt}$ mice vs non-stressed $App^{wt/wt}$ mice; n = 3/each group (Dunnett test). Scale bar = 20 μm.

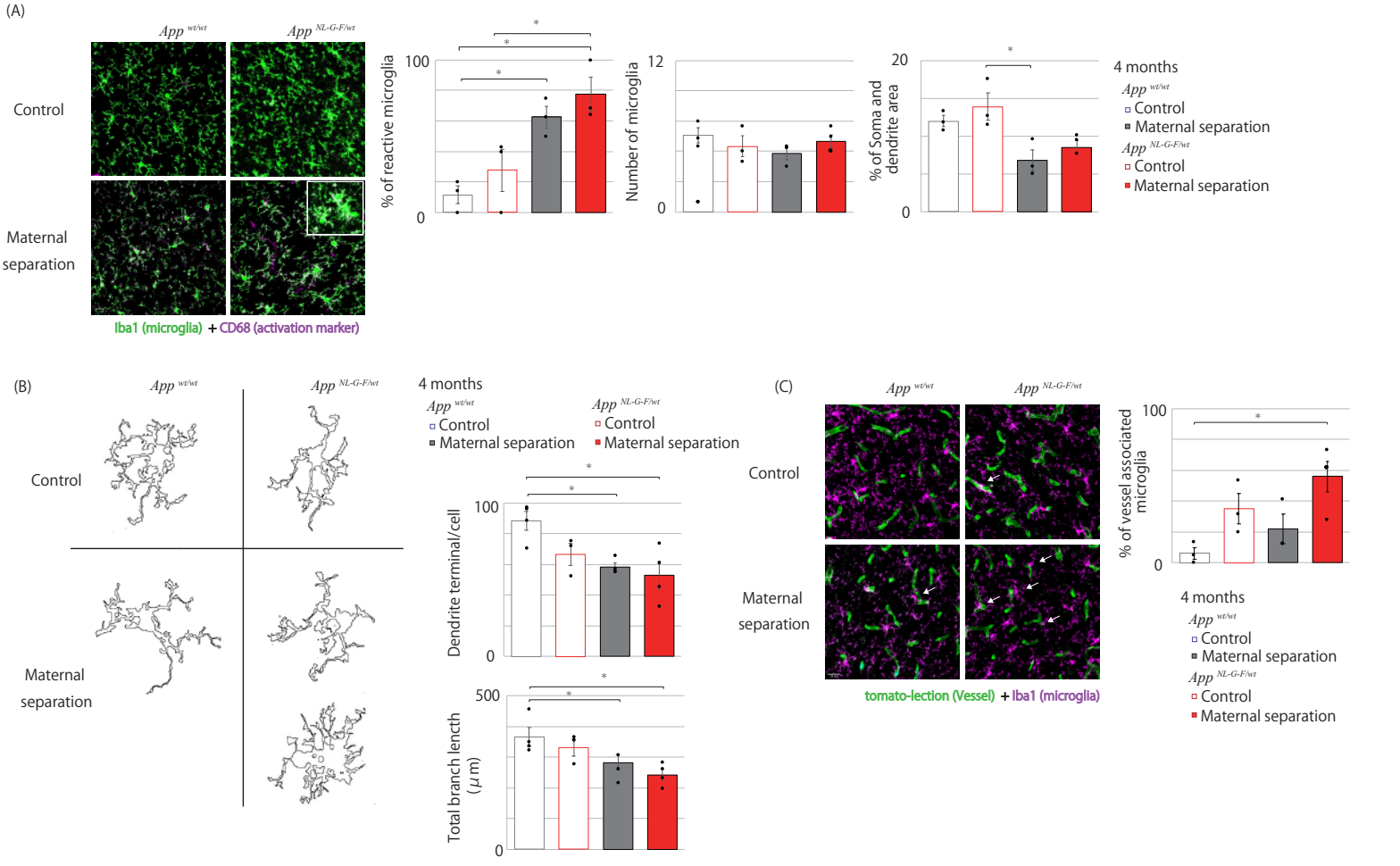

Figure. 4 Maternal separation and genetic factors induced morphological change and activation of microglia.

(A) The morphology and activation of microglia were detected by labelling microglia with Iba1 (green) and labelling activation with CD68 (magenta). Maternal separation induced an increase in activated microglia in *App*$^{wt/wt}$ mice and *App*$^{NL\text{-}G\text{-}F/wt}$ mice. The top right image obtained from a stressed *App*$^{NL\text{-}G\text{-}F/wt}$ mouse shows an example of amyloid plaque-associated microglia. * $p < 0.05$ stressed *App*$^{wt/wt}$ mice vs non-stressed *App*$^{wt/wt}$ mice, * $p < 0.05$ stressed *App*$^{NL\text{-}G\text{-}F/wt}$ mice or non-stressed *App*$^{wt/wt}$ mice. * $p < 0.05$ stressed *App*$^{NL\text{-}G\text{-}F/wt}$ mice or non-stressed *App*$^{NL\text{-}G\text{-}F/wt}$ mice (Tukey-Kramer test). Furthermore, there was lower occupancy of soma and dendrites in stressed *App*$^{wt/wt}$ mice and stressed *App*$^{NL\text{-}G\text{-}F/wt}$ mice. Main effect of genotype, $F_{(1,8)} = 2.7150$, $p = 0.1380$; main effect of stress, $F_{(1,8)} = 15.3801$, $p = 0.0044$; interaction of genotype × stress, $F_{(1,8)} = 0.0164$, $p = 0.9014$, * $p < 0.05$ stressed *App*$^{wt/wt}$ mice vs non-stressed *App*$^{NL\text{-}G\text{-}F/wt}$ mice; n = 3/ Non-stressed *App*$^{wt/wt}$ mice , n = 3/ Non-stressed *App*$^{NL\text{-}G\text{-}F/wt}$ mice , n =3/ Stressed *App*$^{wt/wt}$ mice , n =4/ Stressed *App*$^{NL\text{-}G\text{-}F/wt}$ mice (two-way ANOVA followed by Tukey-Kramer test). Scale bar = 20 μm. (B) Detailed morphological analysis was performed using the ImageJ plugin AnalyzeSkeleton. Images show examples of the outlines of microglia. Maternal separation induced a decrease in dendritic terminals in *App*$^{wt/wt}$ mice and *App*$^{NL\text{-}G\text{-}F/wt}$ mice. * $p < 0.05$ stressed *App*$^{wt/wt}$ mice vs non-stressed *App*$^{wt/wt}$ mice , * $p < 0.05$ stressed A*App*$^{NL\text{-}G\text{-}F/wt}$ mice vs non-stressed *App*$^{wt/wt}$ mice (Dunnett test). Furthermore, there was shortening of the total branch length in stressed *App*$^{NL\text{-}G\text{-}F/wt}$ mice. * $p < 0.05$ stressed *App*$^{wt/wt}$ mice vs non-stressed *App*$^{wt/wt}$ mice , * $p < 0.05$ stressed *App*$^{NL\text{-}G\text{-}F/wt}$ mice vs non-stressed *App*$^{wt/wt}$ mice ; n = 4/ Non-stressed *App*$^{wt/wt}$ mice , n = 3/ Non-stressed *App*$^{NL\text{-}G\text{-}F/wt}$ mice , n =4/ Stressed *App*$^{wt/wt}$ mice , n =4/ Stressed *App*$^{NL\text{-}G\text{-}F/wt}$ mice (Dunnett test). (C) Vessel-associated microglia were detected by microglial labelling with Iba1 (magenta) and endothelial cell labelling with tomato-lectin (green). In stressed *App*$^{NL\text{-}G\text{-}F/wt}$ mice, vessel associated microglia (white arrow) were increased. * $p < 0.05$ stressed *App*$^{NL\text{-}G\text{-}F/wt}$ mice vs non-stressed *App*$^{wt/wt}$ mice ; n = 3/ Non-stressed *App*$^{wt/wt}$ mice , n = 3/ Non-stressed *App*$^{NL\text{-}G\text{-}F/wt}$ mice , n =3/ Stressed *App*$^{wt/wt}$ mice , n =4/ Stressed A*App*$^{NL\text{-}G\text{-}F/wt}$ mice (Tukey-Kramer test).

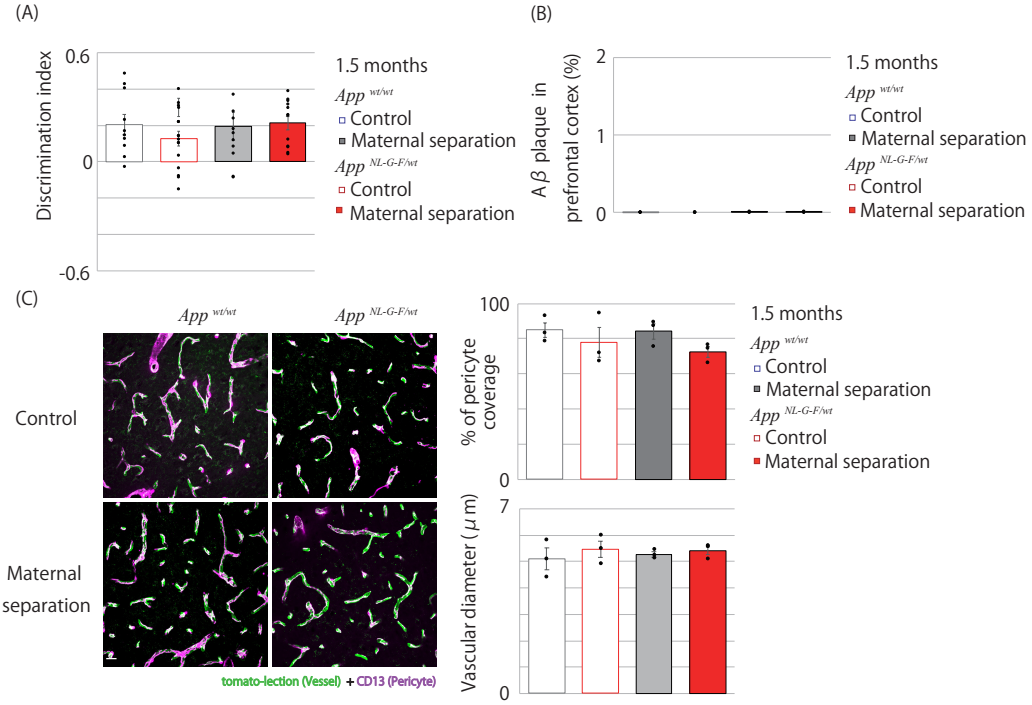

Figure. 5 Alzheimer' s disease like phenotypes did not begin during adolescence in stressed *App*$^{NL\text{-}G\text{-}F/wt}$ mice, and impairment of the vascular system did not begin during adolescence in all groups.

(A) Spatial memory was measured using an object location test. Stressed *App*$^{NL\text{-}G\text{-}F/wt}$ mice showed normal cognitive function. n = 9/ Non-stressed *App* $^{wt/wt}$ mice, n = 11/ Non-stressed *App*$^{NL\text{-}G\text{-}F/wt}$ mice, n = 12/ Stressed *App* $^{wt/wt}$ mice , n = 11/ Stressed *App*$^{NL\text{-}G\text{-}F/wt}$ mice (B) The formation of amyloid beta plaque detected by 82E1-biotin. There was no amyloid beta plaque in stressed *App*$^{NL\text{-}G\text{-}F/wt}$ mice. n = 3/each group

(C) The health of the vascular system was evaluated by tomato-lectin labelling of endothelial cells (green) and CD13 (magenta) labelling of pericytes. All groups showed normal pericyte coverage and a healthy vascular diameter. n = 3/each group. Scale bar = 20 μm.

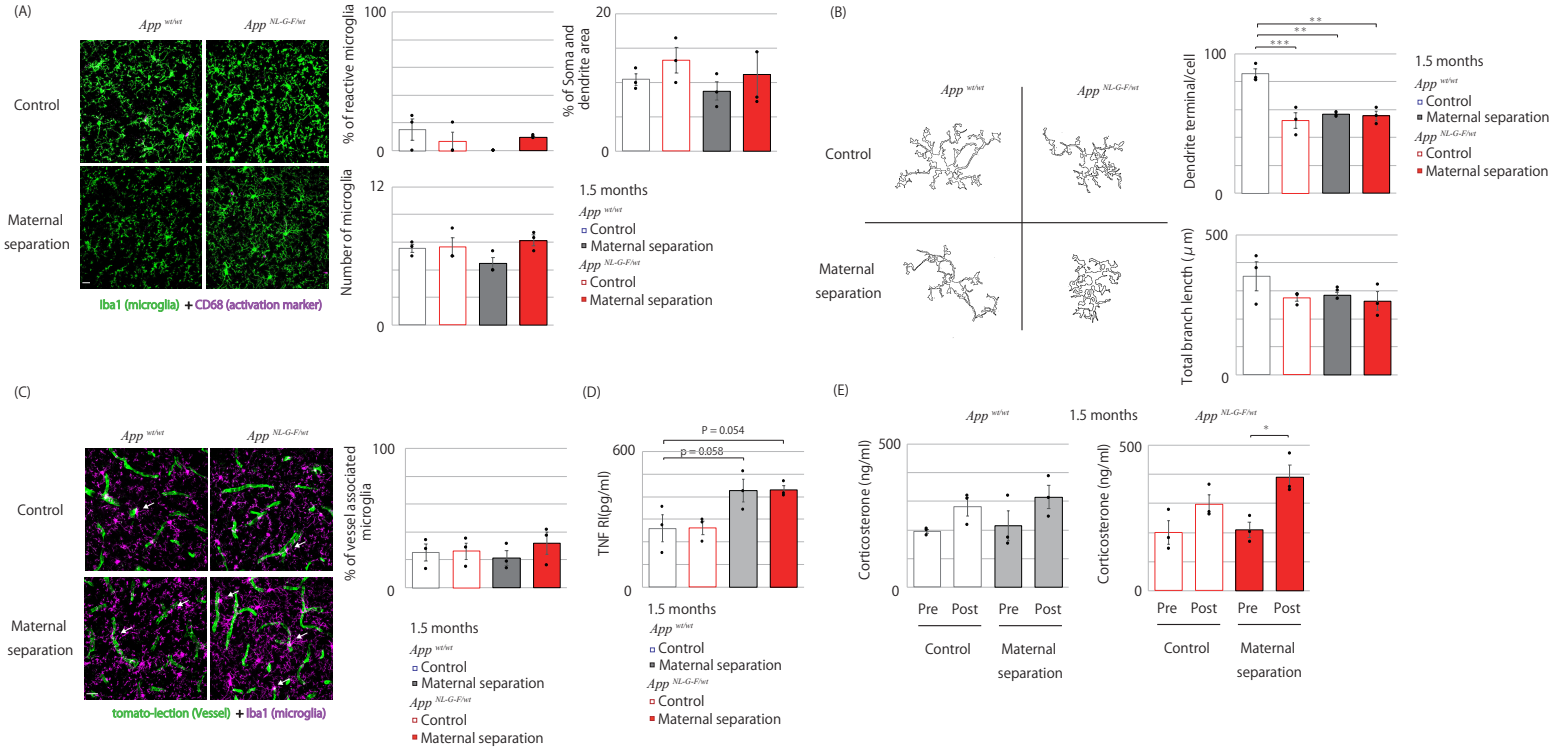

Figure. 6 Maternal separation and genetic factors induced morphological changes in microglia and maternal separation in combination with genetic factors led to abnormality in the stress response during adolescence.
(A) The morphology and activation of microglia were detected by microglial labelling with Iba1 (green) and activation labelling with CD68 (magenta). Increased activation of microglia was not recognized in stressed *App*$^{wt/wt}$ *mice* and stressed *App*$^{NL-G-F/wt}$ mice. n = 3/each group. Scale bar = 20 μm. (B) Detailed morphological analysis was performed using the ImageJ plugin AnalyzeSkeleton. Maternal separation induced a decrease in dendritic terminals in *App*$^{wt/wt}$ *mice* and *App*$^{NL-G-F/wt}$ mice. *** $p < 0.001$ non-stressed *App*$^{NL-G-F/wt}$ mice vs non-stressed *App*$^{wt/wt}$ *mice* , ** $p < 0.01$ stressed *App*$^{wt/wt}$ *mice* vs non-stressed *App*$^{wt/wt}$ *mice* , ** $p < 0.01$ stressed *App*$^{NL-G-F/wt}$ mice vs non-stressed *App*$^{wt/wt}$ *mice* (Dunnett test). (C) The vessel associated microglia were detected by microglial labelling with Iba1 (magenta) and endothelial cell labelling with tomato-lectin (green). The numbers of vessel-associated microglia (white arrow) were similar across the four experimental groups. n = 3/each group. Scale bar = 20 μm. (D) The protein level of TNF-R1 was increased in stressed *App*$^{wt/wt}$ *mice* and stressed*App*$^{NL-G-F/wt}$ mice. $p = 0.058$ stressed *App*$^{wt/wt}$ *mice* vs non-stressed *App*$^{wt/wt}$ *mice*, $p = 0.054$ stressed *App*$^{NL-G-F/wt}$ mice mice vs non-stressed *App*$^{wt/wt}$ *mice.* n = 3/each group (Dunnett test). (E) The response to isolation stress was measured to assess an effect of maternal separation on the HPA axis. *App*$^{NL-G-F/wt}$ mice showed that increased stress caused by maternal separation induced corticosterone release. $F_{(3,8)} = 6.3118$, $p = 0.0167$, * *$p < 0.01$ vs Stressed *App*$^{NL-G-F/wt}$ mice before isolation stress; n = 3/each group (Tukey-Kramer test).